

Research Article

Syeda Safia Hashmi, Muhammad Ibrahim, Muhammad Adnan*, Asad Ullah, Muhammad Nauman Khan, Asif Kamal, Majid Iqbal, Alevcan Kaplan, Nasir Assad, Mohamed Soliman Elshikh, Saeedah Musaед Almutairi, Wajid Zaman*

Green synthesis of silver nanoparticles from *Olea europaea* L. extracted polysaccharides, characterization, and its assessment as an antimicrobial agent against multiple pathogenic microbes

<https://doi.org/10.1515/chem-2024-0016>

received December 6, 2023; accepted March 15, 2024

Abstract: Recent advances in nanoscience and nanotechnology have revolutionized the medical field, particularly in the treatment and prevention of disease. Silver nanopar-

ticles (AgNPs) are considered one of the best supreme and most important nanomaterials with a variety of compulsive nanomaterial having diverse array of multifunctional bioapplications. The current study focuses on the green biosynthesis of AgNPs using polysaccharides extracted from *Olea europaea* leaves. The synthesized AgNPs were thoroughly analyzed and characterized using various spectroscopic and microscopic techniques including, UV-Vis spectroscopy, Fourier transform infrared spectroscopy (FTIR), X-ray diffraction, Energy dispersive X-ray (EDX), and Scanning electron microscopy (SEM). The absorption peak at 440 nm showed a high plasmon resonance band, confirming the formation of green AgNPs by the reduction of Ag^+ ions to Ag^0 . FTIR analysis showed the appearance and extension of different functional groups. The results of EDX and SEM confirmed the synthesis of AgNPs with spherical shape, crystalline structure, and an average size of 64.42 nm. The biosynthesized AgNPs possessed improved antimicrobial activities, indicating the importance of biosynthesized NPs in the pharmaceutical industry. In addition, the biosynthesized AgNPs were biocompatible and exhibited anti-inflammatory activity (86.29%), almost similar to that of a standard drug (87.78%) at a concentration of 500 $\mu\text{L/mL}$. The polysaccharides obtained from *O. europaea* could be considered as effective reducing agent, leading to an environmentally friendly synthesis of stable and biologically important AgNPs with a wide range of applications.

Keywords: AgNPs, biosynthesis, *Olea europaea*, polysaccharides, spectroscopic analysis

* **Corresponding author: Muhammad Adnan**, Department of Chemistry, Islamia College Peshawar, Pakistan, e-mail: muhammadadnan112255@gmail.com

* **Corresponding author: Wajid Zaman**, Department of Life Sciences, Yeungnam University, Gyeongsang-38541, Republic of Korea, e-mail: wajidzaman@yu.ac.kr

Syeda Safia Hashmi: Department of Chemistry, Islamia College Peshawar, Pakistan, e-mail: syedasafia359@gmail.com

Muhammad Ibrahim: Department of Biosciences, COMSATS University Islamabad, Islamabad, Pakistan, e-mail: ibrahimattullah2347@gmail.com

Asad Ullah: Department of Chemistry, Islamia College Peshawar, Pakistan, e-mail: syedasafia359@gmail.com

Muhammad Nauman Khan: Department of Botany, Islamia College Peshawar, Pakistan; Biology Laboratory, University Public School, University of Peshawar, Peshawar 25120, Pakistan, e-mail: nomiflora@uop.edu.pk

Asif Kamal: Department of Plant Sciences, Faculty of Biological Sciences, Quaid-i-Azam University, 45320, Islamabad, Pakistan, e-mail: kamal@bs.qau.edu.pk

Majid Iqbal: Institute of Geographic Sciences and Natural Resources Research, Chinese Academy of Sciences, Beijing China; University of Chinese Academy of Sciences, (UCAS), Beijing 100049, China, e-mail: miqbal@igsnr.ac.cn

Alevcan Kaplan: Department of Crop and Animal Production, Sason Vocational School, Batman University, Batman, 72060, Turkey, e-mail: kaplanalevcan@gmail.com

Nasir Assad: Institute of Chemistry, University of Sargodha, Sargodha 40100, Pakistan, e-mail: nakhan_98@yahoo.com

Mohamed Soliman Elshikh: Department of Botany and Microbiology, College of Science, King Saud University, P.O. Box 2455, Riyadh 11451, Saudi Arabia, e-mail: melshikh@ksu.edu.sa

Saeedah Musaед Almutairi: Department of Botany and Microbiology, College of Science, King Saud University, P.O. Box 2455, Riyadh 11451, Saudi Arabia, e-mail: alsaeedah@ksu.edu.sa

1 Introduction

Nanobiotechnology is a new field in medicine in which nano-sized materials are used for targeted cell or tissue-specific medicinal interventions. The goal of nanotechnology is the development and application of methods to produce nanosystems that can interact at the molecular level with high specificity to achieve maximum therapeutic effects with minimal adverse effects [1]. Nanotechnology has emerged as the most important tool in the bioproduction process of metallic nanoparticles (MNPs). Over the past decades, nanotechnology has made several advances. Compared to other sectors, the importance of this technology in agricultural research is relatively new. The use of nanoparticles (NPs) as nano-fertilizers plays an important role in successful crop production. Used in the appropriate concentration, these nano-fertilizers significantly increase plant growth, crop yield, and plant tolerance [2]. Nowadays, new applications with great technological potential are still being discovered. In the nanoworld, the motto is: smaller size with greater potential. This has led to the creation of NPs in various sizes and shapes.

Due to their small size, large surface area, and other important and unique features, NPs have attracted considerable attention especially in the field of medicine [3]. The synthesis of metal NPs has attracted great interest in the last decade due to their wide range of applications, including crop production [4], antioxidants [1], bio-imaging, diagnostics, bio-sensing, gene therapy, antimicrobials [5,6], and anticancer drugs [7]. Compared to conventional drugs, the higher biocompatibility of NPs ensures site-specific delivery, increasing the efficiency of therapeutics while reducing adverse side effects. Within metal and metal oxide NPs, Silver nanoparticles (AgNPs) have received meticulous attention due to their wide range of biological applications, including anticancer, antimicrobial activity [8,9], antioxidant [10], and medical imaging [11,12].

Several physical and chemical processes can be used to synthesize AgNPs. However, the high production costs and toxicity concerns associated with the above methods paved the way for a highly affordable, reliable, and environmentally friendly green synthesis process [13–17]. In green synthesis, different plant extracts are used as reducing and stabilizing agents to synthesize the AgNPs [18–21]. Although several studies have been reported on the green synthesis of AgNPs using different plant parts, Rehman *et al.* [22] synthesized AgNPs using *Delphinium uncinatum* root and stem extract and investigated its antioxidant, enzyme inhibitory, cytotoxic, and antimicrobial potential [22]. In a study by Widadalla *et al.* [23], green tea leaf extracts were used to synthesize AgNPs. UV-Vis spectroscopy

and Fourier transform infrared spectroscopy (FTIR) were used to analyze the synthesized AgNPs [23].

Antibiotic resistance is a serious public health problem in both emerging and industrialized countries. Antibiotic treatment is severely compromised by the increasing prevalence of diseases that are resistant to many drugs [3,7]. Therefore, it is important to look for other sources of antimicrobial agents, such as plant-based nanomaterials, which contain a variety of bioactive elements that have been shown to have therapeutic properties [7]. It is now widely recognized that the development of environmentally friendly methods for the production of MNPs is an important advance in development. The antibacterial activity of green synthesized AgNPs was evaluated by Widadalla *et al.* [23]. Khader *et al.* [24] synthesized AgNPs from *Phoenix dactylifera* L. seed extract and evaluated *in vitro* anti-inflammatory, anti-arthritic, and anti-proliferative activities without using additional stabilizing or capping agents [24]. Sivakumar *et al.* [25] documented the eco-friendly method of synthesizing AgNPs from the leaf extract of *Andrographis macrobotrys* Nees. Moreover, a range of biological activities were investigated including antibacterial, antioxidant (DPPH and ABTS), cytotoxic (using lung cancer (A549) cell lines), and anti-inflammatory (albumin denaturation and HRBC membrane) [25]. Naik and David [26] performed biosynthesis of AgNPs using *Caesalpinia bonducella* (L.) Fleming leaf extract. The biosynthesized AgNPs were tested for their anti-inflammatory properties using a protein denaturation technique. The anti-cancer efficacy against MCF-7 cells was tested using the MTT assay [26].

The use of medicinal and aromatic plants has increased significantly in recent years, both as traditional remedies and as raw materials for the cosmetics and pharmaceutical industries. The evergreen olive tree (*O. europaea*) is highly valuable as it is one of the several medicinal plants that have been used for hundreds of years and are rich in phenols with beneficial bioactive properties [27]. The olive leaf is naturally resistant to assault by microbes and insects, and the antibacterial effect of the chemicals contained in the olive fruit and olive oil has been the subject of numerous scientific studies. Olive leaves, with their antibacterial characteristics, have long been used in traditional medicine as a means of treating fever and overcoming infections [11]. The biosynthesis of NPs from medicinal plants has recently gained interest due to numerous advantages, including a more environmentally friendly and cost-effective approach. The biosynthesis approach offers the possibility of overcoming the problem of using stabilizer agents to avoid NP aggregation. A range of biological agents have been effectively used in the biosynthesis of NPs, including algae, fungi, enzymes,

bacteria, polysaccharides, oligosaccharides, DNA, and human cell lines [28].

The aim of this study was to synthesize AgNPs using the olive plant through a low-cost and green technology protocol. The green synthesized AgNPs were thoroughly characterized by several spectroscopic and microscopic techniques and their antimicrobial and anti-inflammatory potential was evaluated.

2 Materials and methods

2.1 Plant collection and extraction

The leaves of *O. europaea* were collected and dried at room temperature in the shade and then mechanically ground. The powdered sample (500 g) was soaked in methanol and heated at 90°C for 4 h with constant stirring to wipe out pigments, polyphenols, and monosaccharides. The defatted residue was filtered and the procedure was repeated three times.

2.2 Extraction and de proteinization of polysaccharides

The residue of the methanol extraction was air-dried at room temperature in the shade for 1 day and then added with hot water (80°C) and stirred for 2 h. The liquid filtrate and the solid residue were collected and kept in two separate containers. The pH of the filtrates was adjusted to 7.0 using dilute NaOH solution [29]. Five times the volume of ethanol was added to the filtrate, and after 15 h, the crude polysaccharide was recovered by centrifugation at 6,000 rpm for 20 min. The polysaccharides obtained were deproteinized using the Sevag method. In brief, chloroform and *n*-butanol were added to the crude polysaccharide solution at 5:1 ratio and stirred continuously for 30 min. The resulting mixture was centrifuged at 600 rpm for 15 min, forming a separate layer of polysaccharide and protein. The protein settled as a precipitate and the deproteinized polysaccharide was dried in an oven at 40°C. The deproteinized polysaccharides were characterized using advanced spectroscopic techniques, i.e., UV, FTIR, X-ray diffraction (XRD), and energy dispersive X-ray (EDX) [30].

2.3 Biosynthesis of AgNPs

The AgNPs were synthesized according to the protocol described in literature. In brief, a 4 mM solution of

AgNO₃ in 250 mL of distilled water (DW). Similarly, 0.13 g of polysaccharide was dissolved in 50 mL of DW. To reduce the Ag⁺ ion, 20 mL of AgNO₃ solution was mixed with 20 mL of polysaccharide solution and stirred for 2 h at a temperature of 50°C. After an incubation time of 24 h, the mixture was centrifuged (600 rpm, 20 min) to obtain AgNPs. The NPs were rinsed with 30 mL of DW and dried in an oven at 50°C [31,32].

2.4 Characterization of AgNPs

Different spectroscopic and microscopic techniques were used to determine the properties of the green synthesized AgNPs and polysaccharides. The UV-Vis spectrophotometer was used in the 200 and 800 nm wavelength range to verify the synthesis of AgNPs. After diluting the tiny aliquot in DW, the concentration of pure Ag⁺ ions was usually measured after 3 to 5 h. Polysaccharide and green synthesized AgNPs were analyzed by FTIR spectroscopy in the range of 4,000–500 cm⁻¹ to identify the corresponding functional groups and structural characteristics. XRD was used to study the crystallinity of the polysaccharides and the green synthesized AgNPs, while scanning electron microscopy (SEM) was used to analyze the surface morphology of the green synthesized AgNPs [25]. The elemental composition of the polysaccharides and AgNPs was determined using EDX spectra [33]. The physical dimension of the nanocrystals was determined using the Malvern Zetasizer Nano ZS.

2.5 Antimicrobial activities of polysaccharides and AgNPs

2.5.1 Antibacterial activity

The antibacterial activity was assessed using the protocol described by Khan et al. [34], with few modifications. *Staphylococcus aureus* (ATCC 23235), *Salmonella typhi* (ATCC 14028), *Escherichia coli* (ATCC 10536), and *Pseudomonas aeruginosa* (ATCC 27833) were selected based on their clinical and pharmacological significance. The bacterial strains were cultivated on nutrient broth and incubated at 37°C for 24 h. For antimicrobial activity, nutrient media were prepared by dissolving 15 g nutrient agar in 700 mL of DW and autoclaved at 121°C for 20 min. Inoculum containing 10⁶ CFU/mL bacteria was spread on the culture media using a sterile swab moistened with bacteria containing suspension. A sterile cork borer was used to make the wells and

the samples (5, 10, 15, and 20 µg/L) from a stock solution of 1 mg/mL in DMSO were added to the wells. Control experiments were performed under similar conditions with lincomycin as standard drug. After 30 min of diffusion of the sample and the negative and positive controls, the Petri dishes were incubated at 37°C for 24 h. The diameters of the inhibition zones were measured in millimeters (mm).

2.5.2 Antifungal activity

The antifungal activity was evaluated against, *Alternaria solani*, *Aspergillus terreus*, *Aspergillus niger*, and *Alternaria alternata*. The antifungal activity was used with the exception of potato dextrose agar as a culture medium, while Clotrimazole Topical Solution USP (United States Pharmacopeial Convention) was used as a positive control and the incubation period was 42 h. The antifungal activity was performed using the disc diffusion method [35,36].

2.6 Anti-inflammatory activity

The anti-inflammatory effects of the polysaccharides extracted from *O. europaea*-mediated AgNPs were analyzed by protein denaturation according to a method described in previous studies [34,37] with some minor modifications. To obtain a final volume of 5 and 2.8 mL of phosphate-buffered saline (PBS) (pH 6.4), 0.2 mL of fresh egg albumin and 100–500 µL/mL of polysaccharides extracted from *O. europaea*-mediated AgNPs were mixed. The mixtures were incubated at 37°C for 20 min and then heated to 70°C for 5 min. Absorbance for the reference drug diclofenac sodium (500 µL/mL) was determined in a similar manner. After processing the sample solution, a control solution was prepared by mixing 2.8 mL of PBS (pH 6.4) with 0.2 mL of egg albumin solution and bringing the volume to 5 mL with DW. The turbidity was measured at a wavelength of 660 nm using a UV-Vis spectrophotometer. The percentage (%) inhibition was calculated using the following formula [38]:

$$\text{Inhibition of protein denaturation(\%)} = (\text{Abs}_{660\text{of sample}} / \text{Abs}_{660\text{ of control}} - 1) \times 100$$

2.7 Statistical analysis

Statistical analysis was performed using statistical software including origin and SPSS7.

3 Results and discussion

3.1 UV-visible analysis of polysaccharides and AgNPs

The UV-Vis spectral analysis of the crude polysaccharide solution was performed using a UV-Vis spectrophotometer in the 200–800 nm range and revealed that the less conspicuous peaks at 280 nm indicate the presence of protein and nucleic acid impurities. Figure 1b shows a high plasmon resonance band observed at an absorption peak of 440 nm, confirming the formation of AgNPs by the reduction of Ag^+ ions [26]. Our results were in good agreement with previous literature reports [12,13,39]. The absorption peak at 440 nm indicates the reduction of Ag^+ to Ag^0 in the form of AgNPs in the solution mixture.

3.2 FTIR

The FTIR spectra of the polysaccharides (Figure 2a) show that the peaks at 3343.707, 2920.131, and 2850.909 cm^{-1} correspond to the stretching vibration of the N–H bond, indicating the presence of an amine group. The peaks at 1633.990 and 949.949 cm^{-1} represent the C–H stretching of the aromatic compound and the peaks at 1142.826 cm^{-1} show stretching of the N–H bond, indicating the presence of an aromatic amine. The FTIR spectra (Figure 2b) of the AgNPs show that the peaks at 3368.192 cm^{-1} correspond to

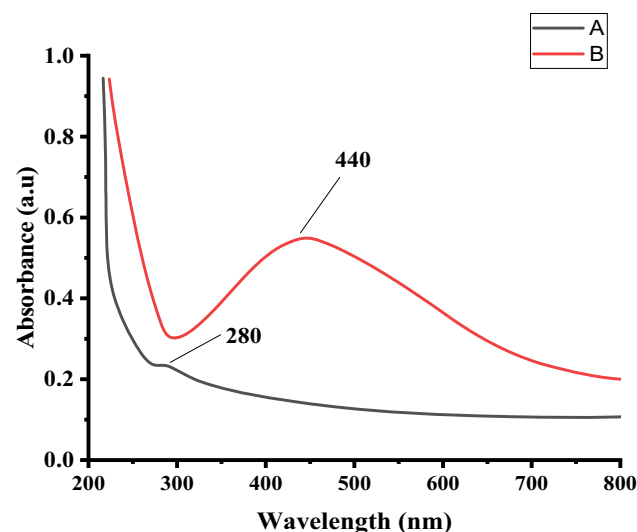


Figure 1: UV-Vis spectra of polysaccharides (a) and their AgNPs (b).

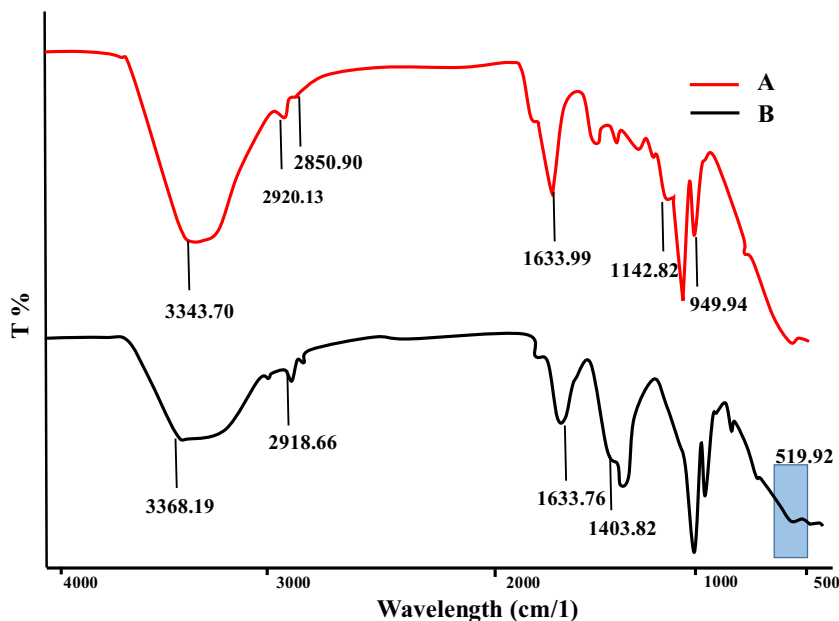


Figure 2: FTIR spectra of polysaccharides (a) and their biosynthesized AgNPs (b).

an O–H bond, indicating the presence of an alcohol group. The peak at 2918.667 cm^{-1} corresponds to the C–H bond, which represents the alkane group. The peaks at 1633.768 and 1403.828 cm^{-1} correspond to C–C and S–O stretching vibrations, indicating the presence of alkene and sulphate groups, respectively [31,40]. The stretching vibration at 519.92 can be assigned to the Ag–O bond [18,41]. The overall FTIR spectrum of AgNPs synthesized with polysaccharides extracted from *O. europaea* leaves showed similarity, though with minor shifts in the positions of the bands indicating the presence of Ag.

3.3 XRD

XRD analysis of polysaccharides and AgNPs (Figure 3) shows the XRD patterns of (a) pure polysaccharides and (b) their biosynthesized AgNPs, to evaluate the purity and crystallinity. Three minor peaks, with 2θ at 24.8 and 31.8 [42], were observed in the XRD plot of the extracted polysaccharide (Figure 3a), while prominent peaks at 2θ values of 38.4 can be observed in the XRD plot of the synthesized AgNPs at 44.97 , 64.45 , and 77.75 are observed, which are assigned to the (111), (200), (220), and (311) diffraction planes, respectively (Figure 3b). These diffractions could be attributed to the cubic structure of the pure Bragg reflection of the face-centered cube structure of the metal powder phase [43]. Two additional peaks in the diffractogram at 2θ values of 27.85 and 32.15 are observed, which

can be attributed to unreduced AgNO_3 . Similar results were reported by Mehta et al. [44].

In this study, the XRD data were used to measure the grain size or crystallite size of AgNPs. The crystallite size was calculated using the Scherrer equation (equation (1)).

$$D = K\lambda \cos\theta, \quad (1)$$

where the Scherrer standard, denoted by K , has a value of 0.9 . The λ -ray, or X-ray, source used in this study has a wavelength of 0.15407 nm . The symbol β stands for the value of the full width at half maximum of the investigated

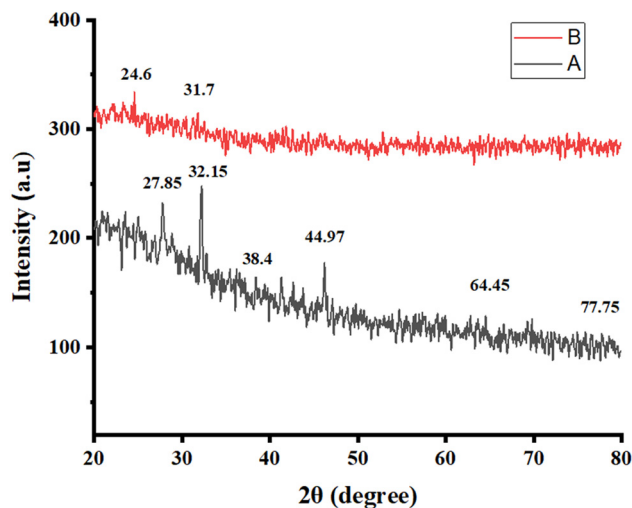


Figure 3: XRD graph of polysaccharide (a) extracted from Olive leaves and their NPs (b).

peaks. Furthermore, the direction of the peak in radians is denoted by θ . The size of the crystallite, determined by examining the XRD peaks, of the sample is 43.41 nm on average.

3.4 EDX and SEM analysis of polysaccharides and its AgNPs

Polysaccharides and green synthesized AgNPs were quantitatively and qualitatively characterized by EDX study [45]. Figure 4c shows the AgNPs produced by polysaccharides; with the silver mass fraction of 15.25%, C mass of 53.74%, and an O of 38.94%, the formation of green AgNPs was confirmed [29]. Figure 4a, and b show the SEM and histograms, respectively. According to the SEM findings, the vast majority of NPs have round forms with an average size of 64.42 ± 2.3 nm [46].

3.5 Zeta sizer

The dynamic dispersion of light (DLS) method was performed to estimate the particle dimension, using the Zeta

sizer Nano ZS (Malvern Panalytical) device. The data presented indicate an average particle size of 71 nm as shown in Figure 4d, which closely agrees with the results of the SEM investigation, as shown in Figure 4a. The DLS size was found to be larger than the crystalline size measured by XRD. Compared to XRD, DLS is a more efficient and cost-effective method for measuring a large number of samples. DLS also provides much bigger numbers, which could be due to the hydrodynamic shell. In addition, the shape and roughness of a particle can change its hydrodynamic shell size [47,48].

3.6 Antimicrobial activities of polysaccharides and AgNPs

3.6.1 Antibacterial activity of polysaccharides and AgNPs

The biosynthesized AgNPs were evaluated for their antibacterial and antifungal potential in comparison to pure polysaccharides extracted from *O. europaea* and standard drugs. For this purpose, a standard protocol for diffusion into wells was applied and different clinically important

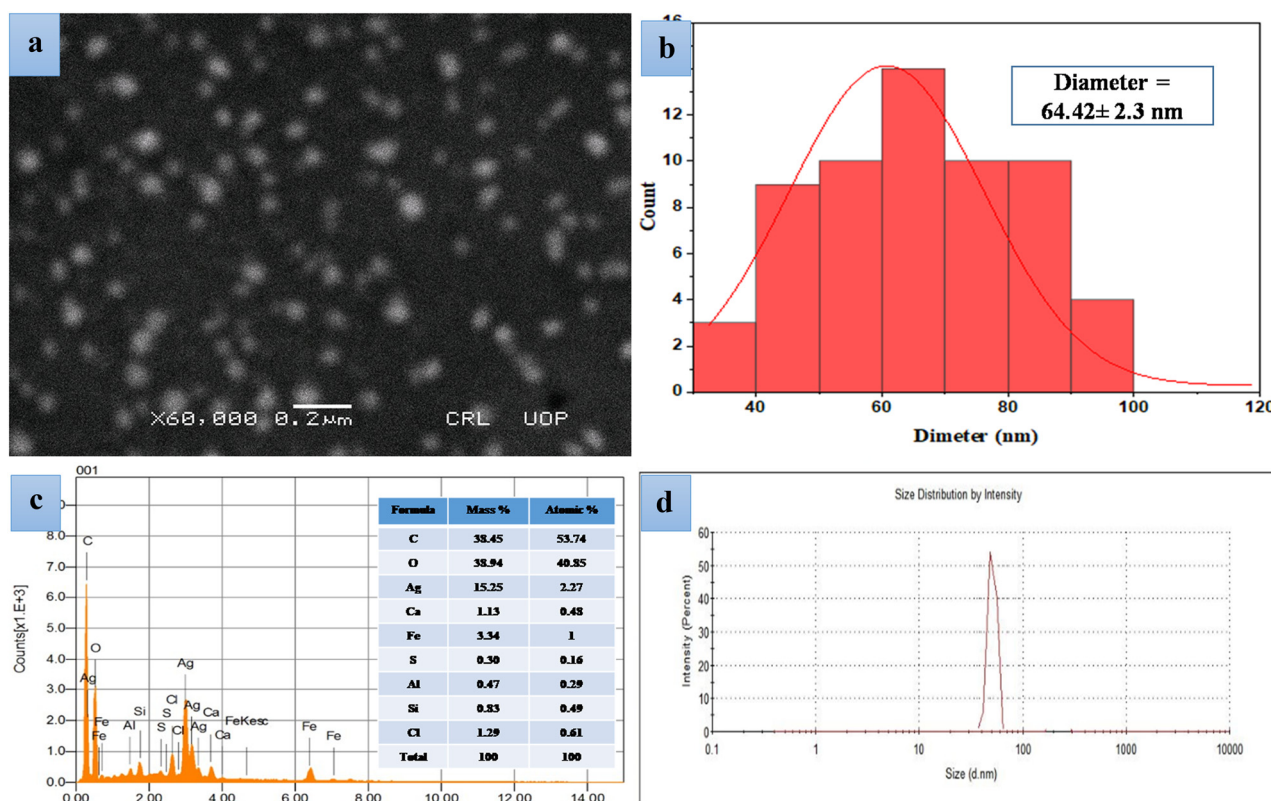


Figure 4: (a) SEM analysis of AgNPs, (b) Histogram, (c) EDX analysis, and (d) particle size distribution of AgNPs synthesized by polysaccharide.

bacterial and fungal species were tested. The results showed that the biosynthesized AgNPs exhibited pronounced antibacterial activity compared to the extracted polysaccharides, with the highest zone of inhibition, i.e., 24 mm, was observed against *Salmonella typhi* (ATCC14028) (Gram -ve bacteria) at a concentration of 20 $\mu\text{g/L}$, while against the bacterial strain *Staphylococcus aureus* (ATCC 23235) (Gram +ve) the AgNPs showed an inhibition of 23 mm at a concentration of 20 $\mu\text{g/L}$ (Figure 5). The current study suggests that the green synthesized AgNPs showed antibacterial activity at different concentrations as shown in Figure 6. The antibacterial activity of the green synthesized AgNPs was greater than that of the pure polysaccharides extracted from *O. europaea* and was compared with the standard drug lincomycin.

3.6.2 Antifungal activity of polysaccharides and AgNPs

The results suggested that both the pure polysaccharide and the biosynthesized AgNPs possessed moderate antifungal activity against the tested species while the AgNPs were surprisingly completely inactive against *A. terreus* at

all concentrations. The highest antifungal potential of the synthesized AgNPs was noted against *A. alternata*, while the extracted polysaccharide with 22 mm zone of inhibition was more active against *A. niger* at a concentration of 20 $\mu\text{g/L}$, as shown in Table 1. The positive controls used in the wells were ciprofloxacin, lincomycin, and fluconazole for antibacterial and antifungal activity, respectively, while the solvent DMSO was used as a negative control.

3.7 Anti-inflammatory activity

Medicinal plants are considered an important resource for novel compounds that may offer therapeutic advantages. For this reason, the study of plants is considered a productive strategy in the search for novel anti-inflammatory drugs that can be used as anti-inflammatory agents in folk medicine. Inflammation has the potential to cause harmful effects, including life-threatening hypersensitivity reactions and chronic organ damage [45]. NSAIDs have the potential to inhibit the denaturation of proteins that act as antigens and induce autoimmune diseases. In some

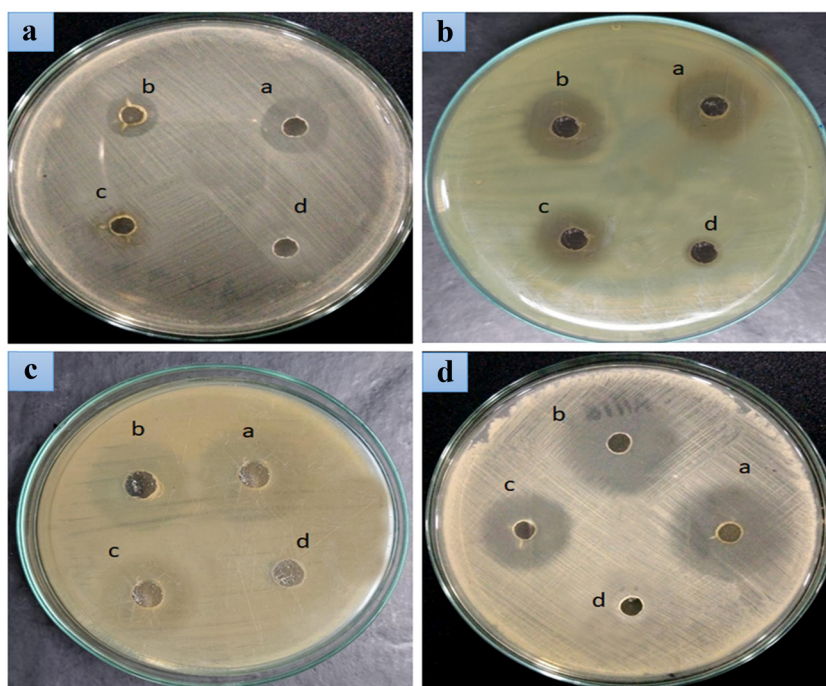


Figure 5: Antibacterial activity of pure polysaccharides extracted from *O. europaea*, AgNPs, and standard drug at concentration of 20 $\mu\text{g/L}$. (A) *Staphylococcus aureus* (ATCC 23235): (a) positive control (25 mm), (b) AgNPs (23 mm), (c) polysaccharides extracted from *O. europaea* (18 mm), and (d) negative control DH_2O (0 mm); (B) *Salmonella typhi* (ATCC14028): (a) positive control (26 mm), (b) AgNPs (24 mm), (c) polysaccharides extracted from *O. europaea* (7 mm), and (d) negative control DH_2O (0 mm); (C) *Escherichia coli* (ATCC 10536): (a) positive control (24 mm), (b) AgNPs (23 mm), (c) polysaccharides extracted from *O. europaea* (16 mm), and (d) negative control DH_2O (0 mm); and (D) *Pseudomonas aeruginosa* (ATCC 27833): (a) positive control (26 mm), (b) AgNPs (21 mm), (c) polysaccharides extracted from *O. europaea* (18 mm), and (d) negative control DH_2O (0 mm).

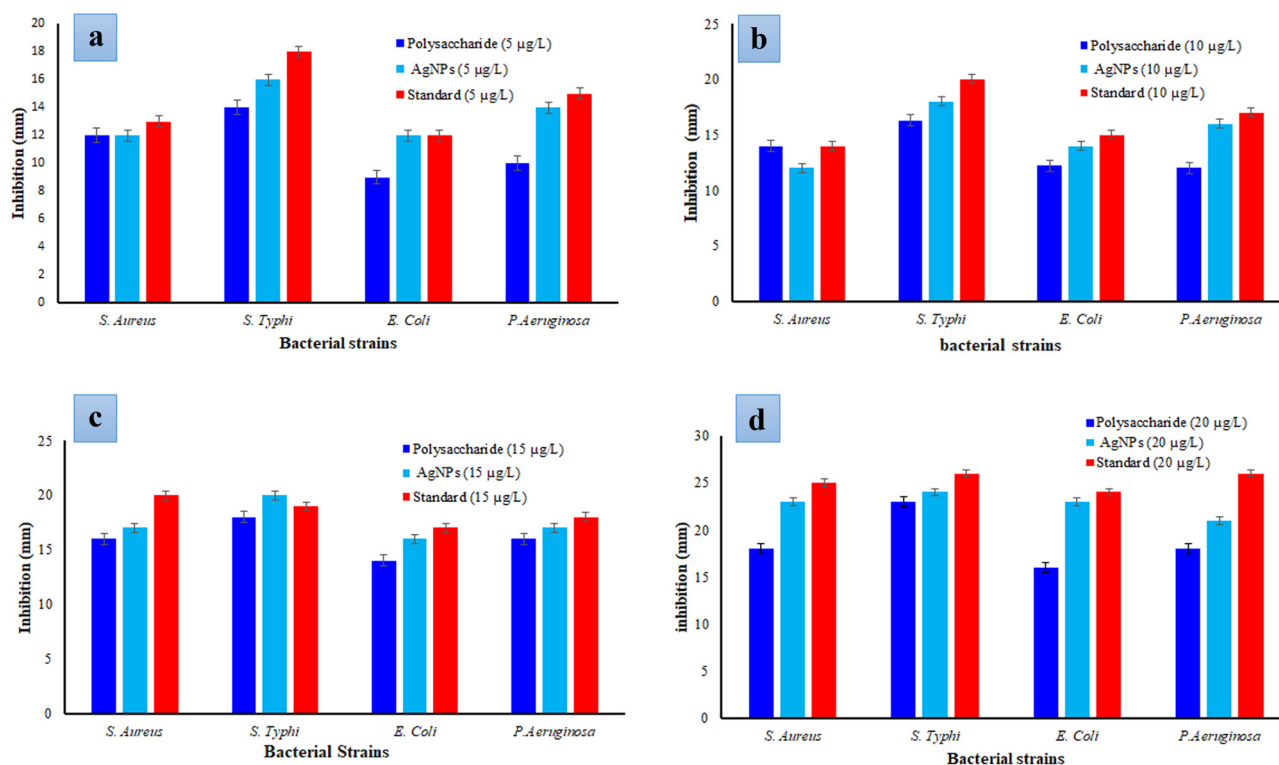


Figure 6: Antibacterial activity of pure polysaccharides extracted from *O. europaea*, AgNPs, and standard drug at concentrations of (a) 5 µg/L, (b) 10 µg/L, (c) 15 µg/L, and (d) 20 µg/L.

Table 1: Antifungal activity of pure polysaccharides extracted from *O. europaea*, AgNPs, and standard drug

S. no	Fungal strains	Zones of inhibition by polysaccharide (mm)				Zones of inhibition by AgNPs (mm)				Zones of inhibition by standard (mm)	
		5 µg/L	10 µg/L	15 µg/L	20 µg/L	5 µg/L	10 µg/L	15 µg/L	20 µg/L	5 µg/L	
1	<i>A. solani</i>	9.6	12.8	14.7	16.4	12.2	14.9	16.8	19.2	30	
2	<i>A. terreus</i>	12.2	14.6	16	18.2	0	0	0	0	35	
3	<i>A. niger</i>	16.4	18.6	20.8	22	8.2	9	9.6	10	38	
4	<i>A. alternata</i>	8	12.9	14.8	16	14.4	16.4	17.8	20.2	35	

inflammatory diseases, such as rheumatoid arthritis, the body responds by denaturing proteins [49]. For this reason, the fact that the investigated polysaccharides from *O. europaea*-mediated AgNPs could stop protein denaturation and reduce inflammation. The dose-dependent anti-inflammatory effect demonstrated in this study was caused by polysaccharides from *O. europaea*-mediated AgNPs, as shown in Table 2. The percent inhibition values of the synthesized AgNPs ranged from 86.29% at the highest concentration (500 µL/mL) to 39.90% at the lowest concentration (100 µL/mL). According to the results of this study, the biosynthesized AgNPs were capped by the secondary metabolites polysaccharides extracted from *O. europaea*. Some secondary metabolites of polysaccharides from *O. europaea*-

mediated AgNPs have been shown to inhibit neutrophils from releasing lysosomal components at the site of inflammation. When proteinases and antimicrobial enzymes stored in lysosomes are released into the extracellular space, they cause more damage to cells and inflammation [50]. Similar results were described by Gwatidzo *et al.* [51]. Our results are also in good agreement with previous literature [52].

3.8 Comparison with literature

A comparison of the previously reported synthesized AgNPs and their applications and sizes with the current study is provided in Table 3.

Table 2: Anti-inflammatory activity of polysaccharides extracted from olive plant and biosynthesized AgNPs

Concentration (μL)	<i>O. europaea</i> (% inhibition)	<i>O. europaea</i> mediated AgNPs (% inhibition)	Diclofenac sodium (500 μL) (% inhibition)
100	13.70	39.90	87.78
200	21.34	51.79	
300	35.31	67.59	
400	39.64	79.87	
500	43.98	86.29	

Table 3: Comparison of the previously reported synthesized AgNPs

Plant source	Plant part	Size (nm)	Applications	References
<i>Cotoneaster nummularius</i> Lindl.	Leaves	122.8	Antimicrobial, wound healing	[41]
<i>Euphorbia royleana</i> Boiss.	Stem	8–200	Control microbial, oxidative stress	[34]
<i>Mimosa pudica</i> L.	Seeds	2–18	Antimicrobial, wound healing	[53]
<i>Olea europaea</i> L.	Fruit	77	Antibacterial, antioxidant	[21]
<i>Olea europaea</i> L.	Leaves	64.4	Antibacterial, antifungal	Current work

4 Conclusion

This study demonstrated a rapid, cost-effective, ecofriendly, and green route for the synthesis of AgNPs using methanol extract from *O. europaea*. The structural and morphological analysis confirmed the biosynthesis of AgNPs from polysaccharides extracted from the olive plant. The polysaccharide acted not only as a reducing agent but also as a stabilizer of the NPs, which made the whole process economical and environmentally friendly. The successful synthesis of AgNPs was determined using various analytical techniques such as UV-Vis, FTIR, XRD, SEM, EDX, and DLS. The biosynthesized AgNPs exhibited improved antimicrobial potential compared to the pure polysaccharides. Furthermore, the biosynthesized AgNPs showed remarkable anti-inflammatory activity. The results demonstrated that the biosynthesized AgNPs exhibited a dose-dependent activity of 39.90–86.29% at a concentration of 100–500 μL/mL. The biosynthesized AgNPs showed more potent anti-inflammatory activity compared to the polysaccharides extracted from the olive plant and are almost similar to the standard drug diclofenac sodium. The results suggest that the synthesized AgNPs can potentially be used in many areas of the pharmaceutical and food industries without causing adverse effects, although a detailed mechanism of action and further biological studies are suggested.

Acknowledgements: The authors extend their appreciation to the Researchers supporting Project number (RSP2024R470), King Saud University, Riyadh, Saudi Arabia.

Funding information: The research was financially supported by the Researchers supporting Project number (RSP2024R470), King Saud University.

Author contributions: Conceptualization: R.S.S.H., A.K., M.I., and M.A.; methodology: S.S.H. and M.I.; software: M.N.K., A.U., and M.I.; validation: W.Z., A.K., N.A., and M.S.E.; formal analysis: W.Z., A., M.H.K., and M.A.; investigation: A.K. and M.I.; resources: S.M.A.; data curation: W.Z., N.A., A.K., and M.I.; writing – original draft preparation: R.S.S.H., A.K., and M.I.; writing – review and editing: W.Z., A.K., and N.A.; visualization: S.M.A.; supervision: M.S.E.; project administration: M.N.K. and W.Z.; funding acquisition: N.A. All authors have read and agreed to the published version of the manuscript.

Conflict of interest: The authors declare no competing interest.

Data availability statement: The datasets generated during and/or analyzed during the current study are available from the corresponding author on reasonable request.

Ethical approval: The conducted research is not related to either human or animal use.

References

[1] Ullah R, Bibi S, Khan MN, Al Mohaimeed AM, Naz Q, Kamal A. Application of bio-inspired gold nanoparticles as advanced

- nanomaterial in halt nociceptive pathway and hepatotoxicity via triggering antioxidation system. *Catalysts*. 2023;13(786):1–24.
- [2] Ul Haq T, Ullah R, Khan MN, Nazish M, Almutairi SM, Rasheed RA. Seed priming with glutamic-acid-functionalized iron nanoparticles modulating response of *Vigna radiata* (L.) R. Wilczek (Mung Bean) to induce osmotic stress. *Micromachines*. 2023;14(736):1–17.
 - [3] Oves M, Rauf MA, Aslam M, Qari HA, Sonbol H, Ahmad I, et al. Green synthesis of silver nanoparticles by *Conocarpus Lancifolius* plant extract and their antimicrobial and anticancer activities. *Saudi J Biol Sci*. 2022;29(1):460–71.
 - [4] Ajmal M, Ullah R, Muhammad Z, Khan MN, Kakar HA, Kaplan A, et al. Kinetin capped zinc oxide nanoparticles improve plant growth and ameliorate resistivity to polyethylene glycol (PEG)-induced drought stress in *Vigna radiata* (L.) R. Wilczek (Mung Bean). *Molecules*. 2023;28(5059):1–19.
 - [5] Javed MN, Bangash SAK, Abbas M, Ahmed S, Kaplan A, Iqbal S, et al. Potential and challenges in green synthesis of nanoparticles: A review. *Xi'an Shiyu Daxue Xuebao (Ziran Kexue Ban)*. *J Xi'an Shiyu Univ*. 2023;19(02):1155–65.
 - [6] Ullah R, Jan SA, Khan MN, Nazish M, Kamal A, Kaplan A, et al. *Euphorbia royleana* Boiss derived silver nanoparticles and their applications as a nanotherapeutic agent to control microbial and oxidative stress-originated diseases. *Pharmaceuticals*. 2023;16(1413):1–20.
 - [7] Zanjage A, Khan SA. Ultra-fast synthesis of antibacterial and photo catalyst silver nanoparticles using neem leaves. *JCIS Open*. 2021;3(100015):1–7.
 - [8] Ishaque MZ, Zaman Y, Arif A, Siddique AB, Shahzad M, Ali D, et al. Fabrication of ternary metal oxide (ZnO: NiO: CuO) nanocomposite heterojunctions for enhanced photocatalytic and antibacterial applications. *RSC Adv*. 2023;13(44):30838–54.
 - [9] Jabbar A, Abbas A, Assad N, Naeem-ul-Hassan M, Alhazmi HA, Najmi A, et al. A highly selective Hg^{2+} colorimetric sensor and antimicrobial agent based on green synthesized silver nanoparticles using *Equisetum diffusum* extract. *RSC Adv*. 2023;13(41):28666–75.
 - [10] Ghaffar S, Abbas A, Naeem-ul-Hassan M, Assad N, Sher M, Ullah S, et al. Improved photocatalytic and antioxidant activity of olive fruit extract-mediated ZnO nanoparticles. *Antioxidants*. 2023;12(6):1–17.
 - [11] Kakakel MA, Sajjad W, Wu F, Bibi N, Shah K, Yali Z, et al. Green synthesis of silver nanoparticles and their shortcomings, animal blood a potential source for silver nanoparticles: A review. *J Hazard Mater Adv*. 2021;1(1):1–12.
 - [12] Oves M, Rauf MA, Hussain A, Qari HA, Khan AAP, Muhammad P, et al. Ismail II. Antibacterial silver nanomaterial synthesis from *Mesoflavibacter zeaxanthinifaciens* and targeting biofilm formation. *Front Pharmacol*. 2019;10(801):1–16.
 - [13] Ahmed S, Ahmad M, Swami BL, Ikram S. Green synthesis of silver nanoparticles using *Azadirachta indica* aqueous leaf extract. *J Radiat Res Appl Sci*. 2016;9(1):1–7.
 - [14] Shinde N, Lokhande A, Lokhande C. A green synthesis method for large area silver thin film containing nanoparticles. *J Photochem Photobiol B: Biol*. 2014;136:19–25.
 - [15] Tippayawat P, Phromviyo N, Boueroy P, Chompoosor A. Green synthesis of silver nanoparticles in Aloe vera plant extract prepared by a hydrothermal method and their synergistic antibacterial activity. *Peer J*. 2016;19(4):1–15.
 - [16] Venkatesham M, Ayodhya D, Madhusudhan A, Veera Babu N, Veerabhadram G. A novel green one-step synthesis of silver nanoparticles using chitosan: Catalytic activity and antimicrobial studies. *Appl Nanosci*. 2014;4(1):113–9.
 - [17] Verma A, Mehata MS. Controllable synthesis of silver nanoparticles using neem leaves and their antimicrobial activity. *J Radiat Res Appl Sci*. 2016;9(1):109–15.
 - [18] Khan ZuR, Assad N, Naeem-ul-Hassan M, Sher M, Alatawi FS, Alatawi MS, et al. *Aconitum lycocotum* L. (Ranunculaceae) mediated biogenic synthesis of silver nanoparticles as potential antioxidant, anti-inflammatory, antimicrobial and antidiabetic agents. *BMC Chem*. 2023a;17(128):1–15.
 - [19] Mohammed AA, Jawad KH, Çevik S, Sulaiman GM, Albukhaty S, Sasikumar P. Investigating the antimicrobial, antioxidant, and anticancer effects of *Elettaria cardamomum* seed extract conjugated to green synthesized silver nanoparticles by laser ablation. *Plasmonics*. 2023;1–14.
 - [20] Rehman I, Gondal HY, Zamir R, Al-Hussain SA, Batool F, Irfan A, et al. Green synthesis: the antibacterial and photocatalytic potential of silver nanoparticles using extract of *Teucrium stocksianum*. *Nanomaterials*. 2023b;13(8):1–14.
 - [21] Ullah S, Khalid R, Rehman MF, Irfan MI, Abbas A, Alhoshani A, et al. Biosynthesis of phyto-functionalized silver nanoparticles using olive fruit extract and evaluation of their antibacterial and antioxidant properties. *Front Chem*. 2023c;11(1202252):1–14.
 - [22] Rehman H, Ali W, Ali M, Khan NZ, Aasim M, Khan AA, et al. *Delpinium uncinatum* mediated green synthesis of AgNPs and its antioxidant, enzyme inhibitory, cytotoxic and antimicrobial potentials. *PLoS One*. 2023a;18(e0280553):1–21.
 - [23] Widatalla HA, Yassin LF, Alrasheid AA, Ahmed SAR, Widdatallah MO, Eltilib SH, et al. Green synthesis of silver nanoparticles using green tea leaf extract, characterization and evaluation of antimicrobial activity. *Nanoscale Adv*. 2022;4(17):911–5.
 - [24] Khader SZA, Ahmed SSZ, Mahboob MR, Prabakaran SB, Lakshmanan SO, Kumar KR, et al. *In vitro* anti-inflammatory, anti-arthritis and anti-proliferative activity of green synthesized silver nanoparticles *Phoenix dactylifera* (Rothan dates). *Braz J Pharm Sci*. 2022;58(e18594):1–12.
 - [25] Sivakumar S, Subban M, Chinnasamy R, Chinnaperumal K, Nakouti I, El-Sheikh MA, et al. Green synthesized silver nanoparticles using *Andrographis macrobotrys* Nees leaf extract and its potential to antibacterial, antioxidant, anti-inflammatory and lung cancer cells cytotoxicity effects. *Inorg Chem Commun*. 2023;153(1):1–13.
 - [26] Naik JR, David M. Green synthesis of silver nanoparticles using *Caesalpinia bonducella* leaf extract: Characterization and evaluation of *in vitro* anti-inflammatory and anti-cancer activities. *Inorg Nano-Metal Chem*. 2023;80:104084.
 - [27] Wang Y, Chinnathambi A, Nasif O, Alharbi SA. Green synthesis and chemical characterization of a novel anti-human pancreatic cancer supplement by silver nanoparticles containing *Zingiber officinale* leaf aqueous extract. *Arab J Chem*. 2021;14(10):1–8.
 - [28] Corciova A, Ivanescu B. Biosynthesis, characterisation and therapeutic applications of plant-mediated silver nanoparticles. *J Serb Chem Soc*. 2018;83(5):515–38.
 - [29] Melkamu WW, Bitew LT. Green synthesis of silver nanoparticles using *Hagenia abyssinica* (Bruce) JF Gmel plant leaf extract and their antibacterial and anti-oxidant activities. *Heliyon*. 2021;7(e08459):1–11.
 - [30] Zangiabadi S, Pourmirzaie A, Naseri F, Ahmadimoghadam A. Floristic status of galoochar juniper forest reservoir, Iran. *Middle-East J Sci Res*. 2012;12(2):141–4.

- [31] Jaast S, Grewal A. Green synthesis of silver nanoparticles, characterization and evaluation of their photocatalytic dye degradation activity. *Curr Res Green Sustain Chem.* 2021;4(100195):1–6.
- [32] Sukweenadhi J, Setiawan KI, Avanti C, Kartini K, Rupa EJ, Yang DC. Scale-up of green synthesis and characterization of silver nanoparticles using ethanol extract of *Plantago major* L. leaf and its antibacterial potential. *South Afr J Chem Eng.* 2021;38(1):1–8.
- [33] Muthulakshmi L, Rajini N, Rajalu AV, Siengchin S, Kathiresan T. Synthesis and characterization of cellulose/silver nanocomposites from bioflocculant reducing agent. *Int J Biol Macromol.* 2017;103:1113–20.
- [34] Khan M, Khan T, Wahab S, Aasim M, Sherazi TA, Zahoor M, et al. Solvent based fractional biosynthesis, phytochemical analysis, and biological activity of silver nanoparticles obtained from the extract of *Salvia moorcroftiana*. *PLoS One.* 2023;18(e0287080):1–26, Ullah B, Hassan S, Khan MN, Razzaq A, Al-Sadoon MK, Wahab S, et al. Phytochemical screening, antimicrobial, antipellucic and antibiofilm activities of the root of alpine medicinal plant (*Arnebia euchroma* (Royle) I.M.Johnst.). *Pol J Environ Stud.* 2023;33(1):425–42.
- [35] Dos Reis CM, da Rosa BV, da Rosa GP, do Carmo G, Morandini LMB, Ugalde GA, et al. Antifungal and antibacterial activity of extracts produced from *Diaporthe schini*. *J Biotechnol.* 2019;294:30–7.
- [36] Hussain I, Salman S, Iftikhar S, Jan S, Akhter J, Ramzan M, et al. Synthesis of Cephadrine metal complexes and its anti-bacterial evaluation. *Sains Malays.* 2018;47(4):749–54.
- [37] Sen S, Chakraborty R, Maramsa N, Basak M, Deka S, Dey B. *In vitro* anti-inflammatory activity of *Amaranthus caudatus* L. leaves. *Indian J Nat Prod Resour.* 2015;6(4):326–9.
- [38] Kyene MO, Droepenu EK, Ayertey F, Yeboah GN, Archer M-A, Kumadoh D, et al. Synthesis and characterization of ZnO nanomaterial from *Cassia sieberiana* and determination of its anti-inflammatory, antioxidant and antimicrobial activities. *Sci Afr.* 2023;19(e01452):1–11.
- [39] Obaid AY, Al-Thabaiti SA, El-Mossalamy E, Al-Harbi LM, Khan Z. Extracellular bio-synthesis of silver nanoparticles. *Arab J Chem.* 2017;10(2):226–31.
- [40] Gudikandula K, Vadapally P, Charya MS. Biogenic synthesis of silver nanoparticles from white rot fungi: Their characterization and antibacterial studies. *OpenNano.* 2017;2:64–78.
- [41] Assad N, Naeem-ul-Hassan M, Ajaz Hussain M, Abbas A, Sher M, Muhammad G, et al. Diffused sunlight assisted green synthesis of silver nanoparticles using *Cotoneaster nummularia* polar extract for antimicrobial and wound healing applications. *Nat Product Res.* 2023;1–15.
- [42] Trilokesh C, Uppuluri KB. Isolation and characterization of cellulose nanocrystals from jackfruit peel. *Sci Rep.* 2019;9(1):1–9.
- [43] Jalab J, Abdelwahed W, Kitaz A, Al-Kayali R. Green synthesis of silver nanoparticles using aqueous extract of *Acacia cyanophylla* and its antibacterial activity. *Heliyon.* 2021;7(9):1–9.
- [44] Mehta B, Chhajlani M, Shrivastava B. Green synthesis of silver nanoparticles and their characterization by XRD. *J Phys: Conf Ser.* 2017;836(012050):1–5IOP Publishing.
- [45] Sangeetha G, Vidhya R. *In vitro* anti-inflammatory activity of different parts of *Pedaliu murex* (L.). *Int J Herb Med.* 2016;4(3):31–6.
- [46] Rodríguez-Félix F, López-Cota AG, Moreno-Vásquez MJ, Graciano-Verdugo AZ, Quintero-Reyes IE, Del-Toro-Sánchez CL, et al. Sustainable-green synthesis of silver nanoparticles using safflower (*Carthamus tinctorius* L.) waste extract and its antibacterial activity. *Heliyon.* 2021;7(4):1–11.
- [47] Barzinjy AA, Azeez HH. Green synthesis and characterization of zinc oxide nanoparticles using *Eucalyptus globulus* Labill. leaf extract and zinc nitrate hexahydrate salt. *SN Appl Sci.* 2020;2(991):1–14.
- [48] Yedurkar S, Maurya C, Mahanwar P. Biosynthesis of zinc oxide nanoparticles using ixora coccinea leaf extract - A green approach. *Open J Synth Theory Appl.* 2016;5:1–14.
- [49] Sharifi-Rad M, Pohl P, Epifano F, Álvarez-Suarez JM. Green synthesis of silver nanoparticles using *Astragalus tribuloides* delile. root extract: Characterization, antioxidant, antibacterial, and anti-inflammatory activities. *Nanomaterials.* 2020;10(12):1–17.
- [50] Govindappa M, Naga S, Poojashri M, Sadananda T, Chandrappa C. Antimicrobial, antioxidant and *in vitro* anti-inflammatory activity of ethanol extract and active phytochemical screening of *Wedelia trilobata* (L.) Hitchc. *J Pharmacogn Phytother.* 2011;3(1):1–5.
- [51] Gwatidzo L, Chowe L, Musekiwa C, Mukaratirwa-Muchanyereyi N. *In vitro* anti-inflammatory activity of *Vangueria infausta*: An edible wild fruit from Zimbabwe. *Afr J Pharm Pharmacol.* 2018;12(13):168–75.
- [52] Kedi PBE, Meva FE, Kotsedi L, Nguemfo EL, Zangueu CB, Ntomba AA, et al. Eco-friendly synthesis, characterization, *in vitro* and *in vivo* anti-inflammatory activity of silver nanoparticle-mediated *Selaginella myosurus* aqueous extract. *Int J Nanomed.* 2018;12(13):8537–48.
- [53] Muhammad G, Hussain MA, Amin M, Hussain SZ, Hussain I, Bukhari SNA, et al. Glucuronoxylan-mediated silver nanoparticles: green synthesis, antimicrobial and wound healing applications. *RSC Adv.* 2017; 7(68); 42900–8.